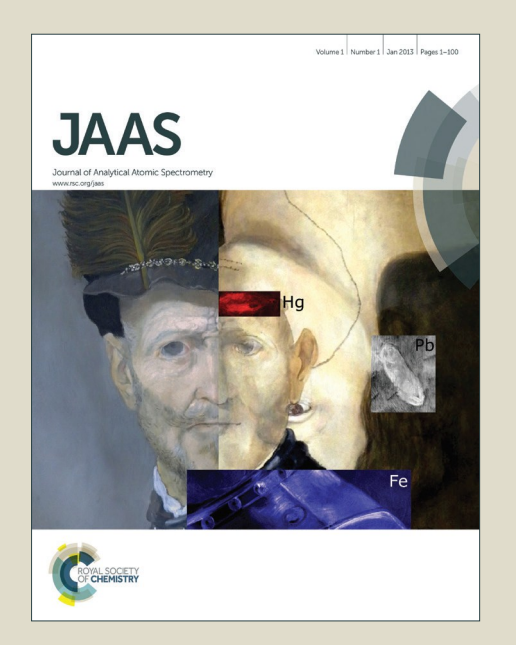
JAAS

Accepted Manuscript



This is an *Accepted Manuscript*, which has been through the Royal Society of Chemistry peer review process and has been accepted for publication.

Accepted Manuscripts are published online shortly after acceptance, before technical editing, formatting and proof reading. Using this free service, authors can make their results available to the community, in citable form, before we publish the edited article. We will replace this Accepted Manuscript with the edited and formatted Advance Article as soon as it is available.

You can find more information about *Accepted Manuscripts* in the **Information for Authors**.

Please note that technical editing may introduce minor changes to the text and/or graphics, which may alter content. The journal's standard <u>Terms & Conditions</u> and the <u>Ethical guidelines</u> still apply. In no event shall the Royal Society of Chemistry be held responsible for any errors or omissions in this *Accepted Manuscript* or any consequences arising from the use of any information it contains.



System Optimization for Determination of Cobalt in Biological Samples by ICP-OES using Photochemical Vapor Generation

Honerio Coutinho de Jesus¹, Patricia Grinberg² and Ralph E. Sturgeon²

Corresponding author: H. C. Jesus; honerio.jesus@ufes.br

¹Universidade Federal do Espírito Santo, Departamento de Química, Av. Fernando Ferrari 514, Vitória, Brazil, 29075-910

²Measurement Science and Standards, National Research Council of Canada, 1200 Montreal Road, Ottawa, Canada, K1A 0R6

ABSTRACT

An optimized photochemical vapor generation (PVG) approach for efficient synthesis of volatile cobalt species is described. Solutions containing Co(II) in a pH 3.3 medium of 50% formic acid were exposed to a source of deep UV (254 and 185 nm) radiation generated within a 19 W flow-through low pressure mercury discharge lamp. Following efficient phase separation, the analyte was transported to an ICP-OES for detection at the 238.892 nm emission line of Co I. Several variables were investigated, including the type of UV lamp and gas-liquid separator, identity and concentration of low molecular weight organic acid, solution pH, sample flow rate and exposure time to the UV irradiation as well as transport gas flow and mode of introduction of sample (continuous or segmented) to the ICP. In continuous mode, an optimum generation efficiency of 42 \pm 2% was achieved with an irradiation time of 10 s, providing a 27-fold improvement in sensitivity compared to pneumatic nebulization and a limit of detection of 0.4 μg L⁻¹ with a precision of 3% at 100 μg L⁻¹. Direct analysis of acid digested biological tissues (NRC TORT-2 and TORT-3) was hampered by strong matrix interferences from the presence of nitrate and other ions which could be circumvented by longer irradiation time and sufficient dilution such that accurate analysis of real samples by the method of additions could be achieved while maintaining high generation efficiency.

INTRODUCTION

Chemical vapor generation (CVG) is a powerful and widely employed sample-introduction technique for determination of trace elements and their speciation in a wide variety of samples. Efficient separation of the analyte and its high transfer efficiency to the detection system confers both high selectivity and sensitivity compared to pneumatic nebulization. This methodology comprises several different strategies, including hydride generation - HG (primarily using sodium tetrahydroborate, NaBH₄), cold vapor generation - CV (Hg, Cd), alkylation (using aqueous compatible alkylating agents, e.g., NaB(Et)₄), halide generation (AsCl₃, SiF₄), oxide generation (OsO₄, CrOCl), oxidation reactions (Cl₂, Br₂, I₂) and metal-carbonyl generation (e.g., Ni(CO)₄). Amongst these, HG relying on BH₄ reductant has emerged as the most widespread approach because of its high sensitivity, fast reaction kinetics, relative robustness, simplicity and cost-effectiveness, yielding good results for determination of classical hydride-forming elements in real samples. In addition, the scope of HG has recently expanded to include generation of a number of transition and noble metals. Other strategies to produce volatile species include electrochemical sonochemical seneration (PVG). Other strategies include electrochemical seneration (PVG).

Interest in PVG has increased in the last decade due to its simplicity, versatility, cost effectiveness, greener footprint and the promise of less severe interferences.¹⁷ This technique is based on the UV photoreduction of elements in solutions containing low molecular weight (LMW) organic acids (normally formic, acetic or propionic acid), resulting in products of photolysis (H₂, CH₄, CO, CO₂, CH₃OH, C₂H₆) and intermediate reducing radicals (*H, *CH₃, *R and *COOH) that promote the formation of volatile species of interest.^{18, 19} In comparison to conventional CVG using BH₄, PVG simplifies chemical manifolds (allowing premixing of the reactants), eliminates the necessity for freshly prepared chemical reductants and generates significantly less H₂, producing more stable signals from plasma-based sources. Several elements have been shown to be amenable to PVG, including the classical hydride forming elements as well as a number of transition metals (Fe, Co, Ni) and non-metals (iodine and bromine), ¹⁹⁻³² substantially enhancing the scope of vapor generation techniques.

Various experimental arrangements have been used to realize PVG, frequently leading to contradictory conclusions. A batch mode of sample processing permits flexible irradiation times to be achieved but generates transient signals and is typically less efficient. Continuous flow or flow injection is more rapid, ^{20, 21} whereas thin-film reactors provide higher efficiencies, especially for less stable volatile species.^{22, 23} A combined spray-chamber/UV photolysis unit has also been studied²⁴ but suffers the inability to control the irradiation time and is functional only over a limited range of sample introduction rates. The use of nano-TiO₂ as a photo-catalyst to improve the PVG efficiencies of some elements, notably Se(VI), opens the field for expanded investigations into improving the kinetics of the PVG process. 18, 25 Although PVG methodologies are routinely optimized for performance once a given experimental system has been selected, less frequently is a comprehensive investigation undertaken to evaluate the impacts of more fundamental components of the system, such as the design of the gas-liquid separator or that of the photoreactor itself (i.e., lamp power, operating wavelength). Qin et al.²⁶ compared different designs of a 19 W flow-through low-pressure mercury discharge lamp for generation of Hg⁰, concluding that the best efficiency was achieved when the sample flowed through synthetic quartz tubing to permit absorption of intense 185 nm radiation from the discharge. Because of its high efficiency, use of this UV source has recently been shown to be advantageous for PVG of a number of transition and non-metals that were difficult to achieve with other sources. 33-39

Zheng et al.⁴⁰ pointed to the possibility that speciation of mercury in a formic acid medium could be undertaken by exposing the sample to either 254 nm radiation for determination of total mercury, or to a visible light source for selective reduction of inorganic mercury. Additional work by Hou et al.⁴¹ utilized a visible LED source to accomplish this, but recent studies by Sturgeon and Luong⁴² point to thermochemical generation as the more likely reason for response from inorganic mercury following exposure to visible radiation. It has also been noted that batch reactors are much less efficient for PVG than their flow system counterparts and, for the latter, the principal contributing factor is the significantly more rapid separation of the volatile species from systems fitted with conventional gas-liquid separators or those that are based on the use of thin-films for sample irradiation^{22, 23} and phase separation.^{32, 33}

More significantly, the majority of the proposed methods could not be readily applied to real samples containing complex matrices, such as digested biological and geological samples, frequently due to the presence of severe interference from oxidants such as the nitrate anion and species that influence radical reactions. This includes both suppressive effects of radical inhibitors, such as oxidants, as well as sensitizers that may be present which enhance reaction kinetics and response. As an example of suppressive effects, Deng et al. 27 investigated the interference arising from several ions on the generation efficiency of Co, with satisfactory recovery only being achieved with relatively clean water samples. Zheng et al. 28 proposed a PVG method to determine Fe by ICP-OES, but samples required either dilution or evaporation of the prepared digest to minimize the serious interference from residual nitric acid arising from the sample digestion process or from the preservative used for water samples. Sensitive determination of Fe was only possible because its high concentration in the CRMs selected for analysis permitted sufficient dilution of the interferent. In subsequent work, Zheng et al.²² investigated several elements using a thin-film reactor, but targeted Fe and Ni to evaluate the accuracy of the proposed approach for the analysis of biological CRMs. Again, evaporation of the nitric acid digestate and a 25-fold dilution with 50% formic acid were needed to eliminate interferences. There was no guarantee that this procedure would be functional for other elements of interest. Noteworthy is that sample concomitants may also give rise to positive interferences, a recent example being the enhancement in sensitivity for PVG determination of lead when either iron or nickel is present in the sample matrix.³⁷ These and other reports suggest that the PVG technique is not yet sufficiently robust for widespread application to real samples, and further investigations are necessary.

Considering the environmental and biological importance of Co, ⁴³⁻⁴⁵ the need to determine low concentrations of this element and the few analytical methods available for this purpose, PVG was herein investigated as an alternative approach and applied to the analysis of biological samples. As noted above, in addition to optimization of the usual analytical variables, the impact of some additional factors, such as the nature of the UV photoreactor, gas-liquid separator design and procedures for sample introduction, were also investigated in an effort to enhance the robustness of the methodology. Although two means were available to accomplish this, either undertaking optimization of experimental variables using a digest of a

real sample matrix, or working with a clean calibration solution and then applying the optimized methodology to real samples, the latter approach was selected in this study. Since the exact composition of real samples is never completely known, optimization with such digests is akin to somewhat working blind. Synthesizing the real sample solutions by systematic addition of known components allows one to immediately evaluate the impact of individual components. Unfortunately, in real samples, the various constituents may even counteract each other or synergistically enhance each other. It must be kept in mind that ultimately the developed method must require calibration for quantitation, which means automatically resorting to the method of additions, or simply dealing with the differences in efficiency as determined by spike recoveries. When optimizing using matrix free calibration solutions, the impact of each of the basic photochemical parameters (reaction medium, UV irradiance and reaction time and temperature) becomes immediately apparent. Optimization with a real sample solution is substantially more difficult, as first attempts at PVG may utterly fail because of unknown matrix interferences, thus slowing development of the entire field.

EXPERIMENTAL

Instrumentation

A Perkin-Elmer Optima 3000 radial view ICP-OES instrument (Waltham, MA, USA) was used for all analytical measurements. The plasma was operated at 1300 W forward rf power sustained with Ar flow rates (L min⁻¹) of 15 for the plasma gas, 0.3 for auxiliary gas and 0.5 for the nebulizer. The Co I 238.892 nm resonance line was used for detection. The PVG system consisted of a low pressure UV mercury discharge lamp in series with a gas-liquid separator (GLS) which delivered the generated volatile Co species directly to the alumina injector of the ICP torch *via* a 25 cm length of 2.5 mm i.d. PTFE tubing of (Alpha Wire Corp., NJ, USA), as illustrated in Figure 1. A cyclonic glass spray chamber fitted with a Conikal concentric nebulizer (Glass Expansion, Pocasset, MA, USA) permitted introduction of water or a standard solution in 1% HNO₃ (for profiling the Co I analytical line) at any time as the spray chamber was mated to the base of the injector via a plastic T-connector which simultaneously accepted delivery of the gas flow from the GLS. All tubing was of PTFE.

Three different designs of UV low pressure mercury discharge lamps were examined. These are illustrated in Figure 2 and comprised a 15 W UV-C germicidal lamp (TUV 15 W/G15 T8, Philips, Holland), a small 3 W pen lamp (Analamp Mercury Ozone Free, $60~\mu W~cm^{-2}$, model 80-1057-01, Claremont, CA, USA), and a unique 19 W flow-through lamp having an internal volume of 0.75 mL (Beijing Titan Instruments Co., Beijing, China) and of a design identical to that used by Qin et al. 26 and similar in principle to that described by Nakazato et al. 46 . Quartz tubes (1.6 mm i.d. x 3.0 mm o.d.) were coiled around both the germicidal and pen lamps so as to produce internal volumes of 8.0 and 1.5 mL, respectively, used to expose the sample to the UV field. The relative intensity of the 254.52 nm Hg line from each lamp was examined, based on measurements made with a compact Jaz Spectral Sensing Suite spectrometer (Ocean Optics Inc., FL, USA). An SR type fiber optic cable ($400~\mu m$ core diameter) was mounted on a rigid 4 mm i.d plastic tube and reproducibly placed 20 cm from the surface of each lamp, permitting an intense spectrum to be acquired without detector saturation. The exterior surface temperatures of the lamps were monitored, along with that of the quartz tube at the point of exit of the irradiated

 solutions, using a Data Logger Thermometer (model HH309, Omega Eng., CT, USA) fitted with a K-type thermocouple.

Sample solutions were introduced in either a continuous or segmented flow mode and upon exit from the photoreactor were directed to a laboratory fabricated GLS (16 cm length and 65 mL inner volume) fitted with a coarse sintered glass frit which supported the irradiated liquid phase. Typically, a 160 mL min⁻¹ flow of Ar entered from below the frit so as to efficiently sparge the volatile species from the irradiated solution and direct them to the ICP, as illustrated in Figure 1. This gas flow was regulated by an external mass flow controller (Brooks Instruments Division, model 5871-B). In addition to this large glass frit GLS, three others, illustrated in Figure 3, were also tested. A 33 cm long (30 mL internal volume) commercially available unit^{32, 33} from Tekran Instruments (for use with their series 2600 automated water analysis system, Toronto, Canada) generated a thin-film of liquid from which efficient, but passive phase separation occurred. A smaller, conventional GLS (6 cm long with 4 mL internal volume), also produced a thin-film from the irradiated sample and also functioned passively. The third GLS was of design similar to that of the larger sparging unit but with reduced dimensions (11 cm long, 10 mL internal volume).

Three peristaltic pumps were used to independently deliver all solutions. The sample pump associated with the emission spectrometer delivered the sample solution to the photoreactor. A Minipuls 2 pump (Gilson, Middleton, WI, USA) eliminated waste from the GLS, and a second such pump delivered water or a standard solution in 1% HNO₃ to the nebulizer as well as evacuated waste from the spray chamber. This configuration enabled the input flow rate of the irradiated solution to be changed while quickly withdrawing waste from the GLS to minimize impact of some foam produced during sparging of the sample. The pumps were operated with Tygon® tubing of various diameters (Elkay Products Inc., Worcester, MA, USA).

A Multiwave 3000 closed-vessel microwave digestion system (Anton Paar, Graz, Austria) equipped with 16 fluoropolymer vessels and ceramic vessel jackets was used for sample preparation. A Perkin-Elmer SCIEX (Elan DRC II) ICP-MS instrument fitted with conventional solution nebulization was used for analysis of Co in post-irradiated sample solutions in order to determine the efficiency of PVG.

Reagents and solutions

All solutions were prepared using 18 M Ω cm deionized reverse osmosis water (DIW) obtained from a mixed-bed ion-exchange system (Nanopure, model D4744, Barnstead/Thermoline, Dubuque, IA). Working solutions were prepared daily by diluting a 1000 mg L⁻¹ stock solution of Co(II) (SCP Science, Montreal, PQ, CA) to 100 μ g L⁻¹ in 1% v/v HNO₃ (for emission profiling of the Co I line) or in a solution of the appropriate LMW acid (for PVG). Solutions of several other metals (Hg, Se, Fe and Ni) were prepared in LMW acid media and used during initial studies to determine optimal instrument conditions.

Nitric acid was purified in-house prior to use by sub-boiling distillation of reagent grade feedstock in a quartz still. Analytical grade hydrogen peroxide (30%, Anachemia Science, Montreal, CA), formic (23 M or 88%, Anachemia), acetic (6.3 M, VWR International, Mississauga, Canada) and propionic acids (13 M, VWR) were used without purification. Solutions of formic acid placed in polyethylene tubes and cooled in an ice bath were pH adjusted by addition of analytical grade solid sodium hydroxide (Sigma Aldrich, Oakville, ON, Canada).

Lobster Hepatopancreas Certified Reference Materials (CRM) TORT-2 and TORT-3 were obtained from the National Research Council of Canada and used to assess the accuracy of the methodology.

Procedure

Test samples of nominal 0.25 g of each CRM were weighed into pre-cleaned Teflon digestion vessels to which 7 mL of sub-boiled HNO $_3$ and 400 μ L of 30% H $_2$ O $_2$ were added. Three procedural blanks were also prepared. The vessels were capped and placed in the microwave oven and subjected to the following heating program: 1) a linear ramp of applied power to 1300 W over 10 min; 2) hold 1300 W for 25 min and 3) cooling utilizing maximum air flow in the microwave cavity until the vessels reached room temperature. After digestion, the acidic solutions were transferred to clean Teflon vessels and concentrated by evaporation to incipient

dryness using a heating block at 95 $^{\circ}$ C in order to remove excess nitrate (interfering ion). The residues were diluted to 10 mL final volume with either 0.5% HNO₃ or a LMW organic acid and stored in precleaned polyethylene screw-capped tubes prior to analysis.

Following ignition and stabilization of the argon plasma and warm-up pf the UV photoreactor, a 1% v/v solution of HNO₃ containing 100 µg L⁻¹ Co was delivered to the nebulizer to permit wavelength profiling of the Co I emission line and to monitor the stability of the spectrometer over the course of the experiments. This procedure was executed using optimized flow rates to the spray chamber (~ 0.8 L min⁻¹ nebulizer gas and 1.3 mL min⁻¹ solution delivery rate). During this step, Ar flow to the GLS was substantially reduced (to 38 mL min⁻¹) to minimize dilution of sample aerosol while at the same time maintaining the entire system flushed with Ar (Figure 1). Following the completion of the wavelength scan and peaking, PVG of Co and other elements of interest was initiated using standard calibration solutions mixed with LMW organic acids. For this step, the nebulizer gas flow rate was decreased to 0.5 L min⁻¹ and Ar flow to the GLS was increased to nominally 160 mL min⁻¹ to achieve effective separation of the volatile species from the liquid phase within the GLS and their transfer to the ICP torch.

Two modes of sample introduction were examined, a continuous flow which generated a steady-state signal but consumed some 10 mL of solution, and a discontinuous or segmented flow mode which permitted optimization of PVG conditions, such as irradiation time, as well as independent variation of the transfer rate of the irradiated solution to the GLS, requiring only about 1 mL of solution to generate a transient signal. In both modes, a peristaltic pump was used to alter the relevant experimental variable under study. Clearly, the flow rate of the sample through the PVG reactor is the same as that for its transfer to the GLS when using the continuous mode of sample introduction but with the segmented flow, these variables could be changed independently.

As noted earlier, several instrumental parameters were optimized to achieve best response. These included rf power, Ar flow rates to the outer, auxiliary and nebulizer channels, the most efficient configuration of photoreactor and GLS, sample irradiation time, solution and Ar flow rate to the GLS, as well as the identity and concentration of the LMW acid and sample pH.

Safety Precautions

All photoreactors were loosely but completely covered with aluminum foil to protect the operator from UV radiation. The use of UV protective eyewear is advised. Adequate workspace ventilation avoided exposure to probable metal carbonyl species formed in these reactions. Waste from the GLS was accumulated in a container for neutralization with soda ash before final disposal.

RESULTS AND DISCUSSION

Previous studies have typically focused on use of a specific UV lamp for the PVG reactor and its coupling to a particular design of GLS with no flexibility for making direct comparisons with alternative designs of both of these components when a single detection system is available. ²⁶⁻³⁶ Furthermore, the impact of several additional parameters is generally not considered, including that of the temperature of the photoreactor on the intensity of the UV lamp (affected by sample flow rate and influencing photon flux) as well as independent supplies of Ar gas to the GLS (required for optimum phase separation and analyte transport efficiencies without causing excessive aerosol formation) and to the nebulizer such that the optimal observation height above the load coil can be achieved. Use of a plastic T-connector at the base of the injector conveniently facilitates this, as illustrated in Figure 1, but this approach is not frequently implemented, ^{22, 28} nor is any consideration given to the effects of the post-irradiation transfer time for the solution to reach the GLS, since continuous sample introduction is most frequently used. Such additional experimental parameters have been investigated in this study.

Following an initial investigation into some of the important experimental factors influencing the PVG technique for generation of several elements (Co, Hg, Se, Fe and Ni) using the different experimental arrangements available for this study, a decision was taken to focus only on Co

because there have been very few published studies of this element and it is of biological importance.

Influence of UV Lamp Characteristics

 Considering the expected higher UV intensity available with the flow-through lamp²⁶ (Figure 2A), this source was used as a benchmark for performance throughout this study, allowing a comparison with two popular UV lamps frequently comprising photoreactors which have been reported in the literature (Figure 2B and C). The temporal variation of intensity of the 254.52 nm Hg line emanating from each source is shown in Figures 4A-C. Due to the U-shaped geometry of the pen lamp, the fiber optic probe sampled emission from the central portion of the discharge (the intensity varies with rotation of the lamp). Use of this lamp for PVG relies on an averaging of the intensity over the length and diameter of the discharge. After stabilization of each lamp (approx. 5 min for UV radiation and 10 min for temperature), water was introduced into each PVG reactor using a peristaltic pump and its impact on temperature and lamp intensity monitored for different flow rates. Each lamp could also be cooled with the use of a small proximity fan and intensity and temperature again followed over time. Lower UV intensity is clearly associated with decreased surface temperatures, highlighting the need to monitor both effects and potentially account for their impact on experimental results. Deng et al.²⁷, for example, reported on the effect of PVG reaction temperature on the fluorescence intensity of generated Co without noting the probable co-variation of the UV intensity from the source lamp.

Figure 4A shows that introduction of water into the flow-through lamp produces a decrease in source intensity as well as temperature at the top of the lamp envelope. Correspondingly, the outlet temperature of the water substantially increases at low flow rates; higher flow rates reduce the sample irradiation and heating times to result in lower temperature rises of the exiting liquid. Correspondingly, high flow rates of water through the lamp decrease the UV intensity by serving as increasingly larger heat sinks. Cooling of the discharge as a result of absorption of heat by the water likely lowers the vapor density of mercury in the discharge and impacts its emission intensity. Cooling is very efficient with this design as the liquid passes

 through the core of the discharge itself. At the highest flow rate of water examined (4 ml min⁻¹), the impact is quite substantial, lowering the intensity of the 254 nm line by 30%. A similar reduction in UV output was also achieved when the lamp was convection cooled by a small fan. The impact of increased sample temperature on the PVG efficiency can be substantial, as has been noted for PVG of Fe²⁸ and Ni²⁹ species, as well as the direct thermochemical reduction of mercury. Fortunately, the flow-through lamp provides for a much more intense and efficient irradiation of samples such that despite significant loss of intensity due to this cooling effect, it remains favorable for PVG of a number of elements. S2-39

These effects are less pronounced with the other two lamps (Figure 4B and C), particularly with the germicidal lamp due to the less intimate contact between the sample coil and the lamp surface as well as the wider spacing between the turns of the surrounding quartz coil which decrease the efficiency of absorption of heat from the lamp by conduction.

The relative performance of the three lamps for PVG was examined based on introduction of a multi-element solution comprising a mixture of 30% formic and 20% propionic acids. This mixture was initially chosen for study based on earlier reports that response from Hg and Se was higher in acetic or propionic acid, whereas that for Co, Ni and Fe was greatest in formic acid. 19, 20, 22, 28, 47 Performance of the various lamps is summarized in Table 1 for samples introduced in this mixture. Care was taken to ensure that the volume of sample solution exposed to the UV field was 0.75 mL in all cases (corresponding to the internal volume of the flow-through lamp). For the germicidal and pen lamps, sections of the surrounding sample coils were thus masked with aluminum foil so as to yield a 0.75 mL internal volume for irradiation. The flow-through lamp exposes the sample to the most intense UV discharge and, expectedly, generally provides for the most efficient PVG of the elements examined. Mercury was exceptional in that the yield of cold vapor from this lamp was compromised with respect to the others, suggesting that losses occurred which could only be explained by assuming a reoxidation of the generated Hg⁰ due to intense production of oxidizing OH radicals. Similar observations have been reported by Qin et al. 25 using an identical flow-through lamp.

Comparison of GLS performance

Apart from the combined UV photoreactor/spray chamber reported by Sturgeon et al., 24 PVG techniques require a distinct GLS to effect separation of the volatile reaction products from the liquid reaction phase. Correspondingly, no performance comparisons have been made using different GLS designs coupled to the same photorector. Moreover, most work has been conducted with low power photochemical reactors which typically cause little gross photolysis (decomposition) of the sample solution. However, due to the high UV intensity of the flowthrough lamp and corresponding direct heat transfer from the discharge, significant evolution of CO, CO₂, H₂ and water vapor accompanies the photolysis of the LMW organic acid solution, ¹⁹ producing bubbles of these gases dispersed along the transport line into which analyte vapor has already begun to partition. Thus, the coupling of passive GLS systems (Figures 3A and B) with the flow-through lamp may be inappropriate, as confirmed by typical signals presented in Figures 5A-C arising from PVG of a multi-element solution containing 30% formic and 20% propionic acids treated with the flow-through lamp and mated to different designs of GLS units. The high efficiency flow-through lamp requires a GLS based on use of a glass frit to actively aid in the rapid and efficient sparging of volatile product, leading to intense signals of satisfactory precision for most elements (RSD < 3% for Co), as shown in Figure 5A. Noisy signals arising from efficient periodic release of high concentrations of volatile metal species into the Ar transfer gas when such bubbles freely escape from the solution as they enter the passive Tekran GLS are evident (Figure 5B). Precision is again improved when the medium glass frit GLS is used (Figure 5C) and although sensitivity is slightly enhanced, overall signal-to-noise is optimal with the larger sparged GLS unit.

Effect of Transfer Gas Flow Rate

 With the flow-through lamp and large glass frit GLS selected as the most appropriate combination of components, a mass flow controller was used to vary the flow rate of Ar to the GLS to establish optimum sparging and analyte vapor transport conditions to the ICP. Analyte emission intensities arising from irradiation of a multi-element solution (prepared according to Table 1) were found to vary proportionally to the Ar flow rate. For Co, response increased 8-fold as Ar flow was increased from 38 to 200 mL min⁻¹. Obviously, this increase is due to the

more efficient mechanical sparging of the volatile species from the liquid phase as the sum of this independent flow of Ar and that introduced via the nebulizer (mixing at the plastic T-connection) was maintained at a constant 0.56 L min⁻¹ for delivery of the analyte vapor to the central channel of the torch; as the GLS flow rate increased, that through the nebulizer correspondingly decreased. This maintains a constant viewing height above the load coil, independent of the flow rate through the GLS, a condition that is not always achieved, ^{22, 28} with the consequence that such optimized parameters actually reflect a compromise amongst several variables as response is influenced by phase separation efficiency, analyte concentration in the carrier gas (extent of dilution at high flows), analyte transport efficiency and its residence time in the plasma (viewing height). Such studies typically report flow rates in the range 0.7-0.8 L min⁻¹, above which higher Ar flow rates cause significant dilution effects and lower response.

Based on use of the flow-through lamp and large glass frit GLS, an Ar carrier flow rate to the GLS of 160 mL min⁻¹ was selected for optimal sensitivity with minimal formation of foam.

Effect of LWM Organic Acids

Based on previous reports, $^{19-37}$ the PVG efficiencies of most elements strongly depend on the type and concentration of LMW organic acid in the solution. Using the above established experimental conditions, solutions containing only Co (II) prepared in formic, acetic and propionic acids at concentrations ranging from 4-60% (v/v) were investigated in detail. Only formic acid provided an analytical response; signals from solutions containing acetic and propionic acids were similar to background intensities, as confirmed in other studies. ^{19, 27} As the identity of the volatile Co species has been reported to be principally cobalt tetracarbonyl dihydride, $Co(CO)_4H_2$, ¹⁹ the efficiency of photochemical generation of H and CO radicals from formic acid appears to be substantially greater than from acetic and propionic acids. After an abrupt increase in signal intensity in the presence of 4-10% formic acid, PVG response from solutions of 500 μ g L⁻¹ Co (II) continued to increase at a lower, but linear rate, from some 7000 cps at 10% to 28000 cps at 60% formic acid.

These observations contrast with the report by Deng et al.²⁷ who established a maximum efficiency in 4% formic acid; similarly, Grinberg et al.¹⁹ selected 5% formic acid as the generation medium so as to minimize deposition of carbon onto the cones of the ICP MS used for detection. These differences may arise as a consequence of the different experimental setups (Deng et al.²⁷ used a 15 W germicidal lamp coupled to a small GLS), or different detection techniques, such as atomic fluorescence, which is prone to quenching if the composition of the gas phase from the GLS contains significant concentrations of molecular species.²⁷ The latter (CO, CO₂, H₂) arise from photolysis of the formic acid and will substantially increase as the acid concentration increases. Additionally, absorption by formic acid in the deep UV is intense and the depth of penetration of 254 nm radiation into the irradiated solution is extremely short at high acid concentrations, possibly decreasing the yield. However, with a small diameter synthetic quartz line transporting sample through the discharge of the flow-through lamp, this is much less likely to present an impediment to efficient formation of reducing radicals.

Before introduction of samples into the PVG system, the Co emission line profile was scanned while nebulizing a 1% solution of HNO₃ containing 100 μ g L⁻¹ Co (II), yielding a typical response of 1350 cps. Processing a 50% formic acid solution containing 500 μ g L⁻¹ Co (II) through the PVG system generated a signal of 24000 cps, a 4-fold enhancement in relative response. The PVG system proves advantageous over pneumatic nebulization (1% HNO₃) only when the concentration of formic acid in a non-pH buffered medium is greater than 15%. Response from solutions containing 100 μ g L⁻¹ Co (II) were 6-fold higher (in non-pH buffered 50% formic acid) than that obtained by Zheng et al.²² using the same ICP spectrometer for detection.

Effect of Sample pH

 Several authors have noted an influence of pH on the PVG reduction of metal ions and consequent generation of volatile alkylated or hydrogenated compounds.^{22-23, 28, 39, 47-50} Low efficiency may arise if the reaction medium is too acidic as re-dissolution of the element may occur if the generated analyte is not quickly separated from liquid phase. If the solution is too basic, cogenerated hydroxyl radicals may facilitate oxidation reactions or an insoluble hydroxide

may form. Zheng et al.²⁸ concluded that the generation of volatile iron compounds (as the pentacarbonyl) was higher from a 50% formic acid solution that is buffered in the pH range 2.0 - 3.0. Satisfactory response was also obtained for As, Sb, Bi, Se and Te in the pH range 0 to \sim 5.²² Guo et al.^{47, 48} obtained no signal for Se at pH > 5. Vieira et al.⁴⁹ reported good results for reduction of Hg²⁺ and CH₃Hg⁺ in the pH range 2-6. Guo et al.⁵⁰ reported that volatile Ni species was favored in a buffered system in which the pH is stable before and after the photochemical reaction, with best results in a mixture of 23 M formic acid and 0.5 M sodium formate.

The effect of sample pH on generation of volatile Co species was investigated using different concentrations of pH buffered solutions of formic acid prepared through the addition of increasing amounts of solid NaOH. This procedure avoids any concurrent variation in the total concentration of formate anion (formic acid + formate anion). Deng et al.²⁶ conducted similar experiments but changed the pH by adding sodium formate, thereby also altering the concentration of formate anion, which may itself influence the photogeneration process.

Figure 6 illustrates results using different concentrations of formic acid buffered with NaOH. All solutions contained 100 μ g L⁻¹ Co (II). Several initial experiments conducted to determine the influence of pH resulted in an ~10% higher intensity for Co emission when water was simultaneously nebulized into the ICP (pumped at 1.3 mL min⁻¹) so as to produce a conventional "wet" plasma (Figure 1). As with many laser ablation-ICP tandem sample introduction systems, use of a wet plasma may promote atomization and excitation due to the high thermal conductivity of generated hydrogen assisting with heat transfer from the outer plasma region.^{51, 52} For this reason, all subsequent experiments were performed using "wet" plasma conditions whose impact is evident from data presented in Figure 6. A similar enhancement occurred at all formic acid concentrations examined. Best response was established near pH 3.3. As the pH of unbuffered 50% formic acid is ~1.0, a 6-fold enhancement in PVG efficiency is realized at pH 3.3. This pH zone is achieved for the condition $C_a/C_b \sim 1.7$, similar to that used by Deng et al.²⁶ (0.93 M formic acid and 0.40 M formic anion, $C_a/C_{bn} = 2.3$).

Influence of Sample Flow Rate

With a continuous mode of introduction, sample flow rate not only determines the irradiation time, i.e., UV radiation dose received and the PVG efficiency, but also the rate of mass transfer of the irradiated solution to the GLS and ultimately of analyte to the ICP. Hence, for a given PVG and GLS efficiency (i.e., independent of irradiation time), response should increase linearly with sample flow rate. If the efficiency is dependent on the irradiation time and phase separation efficiency is flow rate dependent, response will be a convolution of all three effects. Typically, the irradiation time in the PVG system is changed by altering the sample flow rate. Thus, for a continuous mode of sample introduction, the response curve is expected to exhibit an optimum, likely limited at low flow rates by the flux of sample delivered to the GLS, and at high flow rates by the residence time of the solution in the UV field which, in turn, governs the extent of the reaction as well as the potential efficiency of the phase separation process. For example, volatile species of Hg and iodine can be generated within less than 10 s exposure to even the lowest power UV sources, whereas tens of seconds are required for the hydrideforming elements (e.g., Se, Te, Sb, Bi, As) and 2-3 min for several transition metals. 19, 27-31, 50 As irradiation time is increased in the fixed volume flow-through lamp, photolysis products such as CO, CO₂ and H₂ accumulate as numerous expanding bubbles in the photoreactor, capable of expelling the solution into the GLS prior to achieving the needed optimum exposure to the irradiation field. This can result in a partial loss of sample and signal. A further problem associated with longer UV exposure time is the simultaneous decomposition of intermediate or product analyte species, as noted above and reported by Gao and Yin for Hg. 53, 54 Additionally, high solution flow rates enhance the cooling of the source, can decrease the UV intensity from the lamp (cf. Figure 4A) and possibly further affect the total photochemical dose available for absorption by the sample.

The influence of sample flow rate on Co response was investigated using both 30% and 50% formic acid buffered to pH \sim 3.5. Consistent with the data in Figure 6, response in 50% formic acid is some 15% higher, and in both media the signals increase with sample flow rate over the range 0.56 to 5.6 mL min⁻¹, nearly linearly at low flow rates (0.56 to 3.3 mL min⁻¹) and thereafter with decreasing proportionality. Thus, the principal factor responsible for the enhanced Co signal is increase in mass flux of Co species delivered to the GLS and plasma. It is evident that even at a flow rate of 5 mL min⁻¹, the irradiation time (10 s to transit the 0.75 mL

 internal volume of the lamp) is sufficient to generate a good yield of volatile Co species due to the high UV intensity available with this lamp. This observation contrasts with those of Grinberg el al.¹⁹ and Deng et al.²⁷ who reported an initial increase in response with sample flow rate followed by formation of a plateau, likely a consequence of the lower intensity sources available in their studies. A nominal sample flow rate of 3.4 mL min⁻¹ was selected and used for all further investigations as this appears to be the maximum flow rate beyond which either the generation efficiency begins to decrease due to insufficient irradiation time, or the GLS process becomes inefficient and quantitative transfer of the analyte from the liquid phase is not achieved. Data introduced below, in Figure 8B, suggest that quantitative transfer of species from the liquid to gas phase is readily accomplished even at flow rates of 5 mL min⁻¹ to the GLS, leading to the conclusion that sample flow rates exceeding 3.4 mL min⁻¹ through the photoreactor do not permit sufficient irradiation time to drive the photoreaction to completion, or at least to a significant degree.

Using optimal pH conditions (~ 3.3) and a sample flow rate of 3.4 mL min⁻¹, the signal intensities arising from each of the three lamps was re-examined, introducing only a single element solution of Co (II). Table 2 summarizes results; the flow-through lamp provides significantly greater (10-fold) sensitivity than the other two lamps. As noted earlier, the pen and germicidal lamps can compensate for this difference in efficiency when a larger irradiated volume or longer UV exposure time are applied. The ease of implementing such conditions justifies the frequent use these inexpensive commercial lamps.^{20, 24, 27, 47, 49}

Central Composite Design

Considering the significant influence of the concentration of formic acid, solution pH and sample flow rate on Co response, as well as any potential synergistic effects amongst then, a factorial design using central composite design⁵⁵ was performed to confirm the best conditions for operation of the PVG system. These three factors were combined in 5-levels (- α , -1, 0, +1, + α ; α =1.68) using an adequate experimental matrix which required performing 18 experiments (2³ + 2x3 + 4). The chosen experimental central points were 30% formic acid concentration, pH= 3.15 and sample flow rate of 2.5 mL min⁻¹.

The significance of the effects of the variables and possible interactions amongst them was verified by applying analysis of variance (ANOVA) and constructing Pareto charts using Statistica 8.0 software (StatSoft Inc., OK, USA). No significant interaction amongst the three factors (P<0.05) could be discerned from the Pareto analysis. After elimination of these interactions, the design was repeated and significance was evident for pH (quadratic adjustment best) and formic acid concentration (linear adjustment best). The standardized Pareto chart effect indicated sample flow rate was not significant. Figure 7 illustrates the direct influence of the formic acid concentration and pH on Co response for continuous mode sample introduction. Coherence could be observed between the results of this design and those from earlier experiments undertaken by univariate analysis. As an example, for a given sample flow rate, response from Co is largest in the pH range 3.0 - 3.5, increasing with the formic acid concentration in a nearly linear fashion.

Evaluation of segmented mode of sample introduction

 To independently evaluate the impact of UV irradiation time and sample flow rate to the GLS on Co response, a segmented mode of sample introduction was configured. As the internal volume of the flow-through lamp is 0.75 mL, this volume of sample was introduced into a small receptacle to facilitate its quantitative transfer to the photoreactor at various flow rates. The sample plug was bracketed with 100 µL aliquots of water to ensure no loss of volatile Co species (through bubble formation) during selected periods of irradiation. After a defined UV exposure time, the sample was transferred to a 2 mL internal volume PTFE holding line installed between the lamp and the GLS. This permitted subsequent transfer of the irradiated solution to the GLS using an independent flow rate (equal to or different from the sample introduction rate). Both peak height and area (recorded and manually integrated) of the resultant transient signals were monitored. After analysis of each sample aliquot delivered to the GLS, all liquid was evacuated from the system via a second peristaltic pump before a new aliquot of sample was introduced. Results are presented in Figure 8.

Figure 8A illustrates the effect of irradiation time (by changing the sample delivery flow rate to the PVG) while independently delivering a constant and high flux (4.3 mL min⁻¹) of the

 photolysed sample from the holding line to the GLS and thence to the ICP. A nearly constant response is achieved when the irradiation time exceeds 80 s (flow rate < ~0.5 mL min⁻¹) for both peak height and area. This is consistent with the plateaus reported by Grinberg et al.¹⁹ and Deng et al.²⁷ who used continuous sample introduction and a different PVG set-up. The data may suggest a small reduction of integrated response for long irradiation times (very low flow rates), possibly due to decomposition of the Co carbonyl and its reabsorption into the solution prior to delivery to the GLS, but within the precision of measurement this cannot be definitively discerned.

Data presented in Figure 8B confirm the impact of rate of mass transfer or flux of the irradiated solution to the GLS for a given irradiation time (83 s, equivalent to use of ~0.5 mL min⁻¹ sample delivery to the lamp). Due to the severity of asymmetric shape of the transient signals when flow rates of post-irradiated sample delivered to the GLS were below 1.5 mL min⁻¹ (i.e., significant noise superimposed over a long tail), it was not possible to accurately manually integrate these signals and hence data is presented only for the higher flow rates. Nevertheless, it is evident that the peak height increases proportionately to the rate of delivery of sample to the GLS whereas integrated response appears to be constant, as it simply reflects a measure of the total number of atoms of Co delivered to the GLS for the selected sample volume. For a fixed irradiation time, the efficiency of the GLS is independent of the rate of delivery of sample and there are no losses of Co through decomposition processes in the liquid phase over a typical 2 min period in the holding line. This suggests that the potentially slight decrease in intensity of signals presented in Figure 8A at long irradiation times is due to the influence of the UV field; once in the holding line, the sample is no longer exposed to radiation and the continuous generation of the powerful OH oxidizing radical.

In summary, analysis utilizing continuous mode sample introduction convolutes the effects of irradiation time with that of gas-liquid phase separation in the GLS. High flow rates enhance the flux of atoms to the plasma, but potentially at the risk of inefficient residence time in the PVG reactor as well as efficiency of phase separation whereas low flow rates decrease the flux to the GLS but may enhance PVG efficiency (e.g., Fe). The flow-through lamp promotes efficient irradiation (not only at 254 nm, but also at 185 nm), providing enhanced rates of photolysis

such that significantly shorter irradiation times can be utilized (e.g., 10 s compared to several minutes required for other transition metals when less efficient photoreactors are used^{19, 20, 27-29}), allowing advantage to be taken of high mass fluxes to the detector.

Generation Efficiency

 The PVG efficiency of cobalt in the buffered system was estimated by comparison of the concentration of Co (II) in the waste solution exiting the GLS with that fed to the PVG reactor. A 100 μ g L⁻¹ solution of Co (II) in pH 3.5 buffered 50% formic acid subjected to PVG under optimized conditions (sample flow rate = 3.4 mL min⁻¹, Ar flow to the GLS= 160 mL min⁻¹, flow-through lamp and large GLS) was used for this purpose. Comparison of response derived by reintroducing the collected waste into the PVG system does not result in a satisfactory comparison because photolysis of the feed solution may alter the PVG efficiency of the collected waste. Additionally, direct analysis of solutions by pneumatic nebulization with ICP-OES detection is impossible as the high concentration of formic acid causes extinction of the plasma. Thus, the feed and post-irradiated solutions were diluted 100-fold in 1% HNO₃ and analyzed by solution nebulization with ICP-MS detection. The generation efficiency was determined to be 42 \pm 2%, the highest reported for Co by PVG. This value is twice that obtained by Deng et al.²⁷ who used a 15 W UV germicidal lamp for their studies.

Figures of merit

Analytical figures of merit for Co are summarized in Table 3. The signal from a 100 μ g L⁻¹ solution of Co (II) in pH 3.0-3.5 buffered 50% formic acid was typically 37000 cps, 27-fold higher than realized with pneumatic nebulization of a 1% HNO₃ solution of Co(II) at the same concentration (typically yielding 1350 cps with the Optima radial view instrument). A method detection limit (LOD) of 0.4 μ g L⁻¹ for Co is estimated on the basis of three times the standard deviation (n =10) of the Co concentration obtained from the corresponding method blank. A similar LOD was obtained based on the blank arising from the microwave digestion of the biological tissue (TORT CRM). Although Deng et al.²⁶ reported a generation efficiency of only

 23% compared to 42% in this study, their LOD was superior (0.08 μ g L⁻¹ Co) because a more sensitive atomic fluorescence method of detection was used.

Interferences

Previous studies have investigated interferences from common ions (transition and noble metals and anions) in PVG systems. ^{22, 26-29} Zheng et al. ²⁸ concluded that signal suppression of Fe arose primarily because of the acidity of the reaction medium (re-dissolution of intermediate iron) as well as to the presence of nitrate anion (concurrent reaction with organic radicals, or in special cases, co-precipitation as colloids). Apart from nitrate, chloride may also cause interference with PVG, as noted for Ni. ²⁹ Deng et al. ²⁷ also reported significant interferences on Co, mainly due to some hydride-forming elements, which forced them to restrict their proposed methodology to the analysis of simple water samples.

Considering the possible applicability of this methodology to the analysis of Co in biological samples (CRMs) and a desire to avoid the necessity of evaporating digested sample solutions (to reduce or eliminate nitrate anion concentrations), the influence of various concomitant ions was investigated. Iron and Cu were selected due to their high concentrations in biological tissues and nitrate for its presence as a result of microwave assisted acid digestion. These studies were performed using the segmented mode of sample introduction because an earlier suite of experiments did not yield net signals for real samples (digested biological tissue CRM) with continuous mode, as discussed below.

Figure 9 illustrates the impact of nitrate concentration on Co response. Three experiments were performed over different days to confirm reproducibility. Aliquots of 1 mL of 100 μ g L⁻¹ Co (II) in pH 3.5 buffered 50% formic acid containing increasing concentrations of nitrate (derived from additions of 5% HNO₃) were introduced into the flow-through lamp at a rate of 1.1 mL min⁻¹; the effluent was collected in a 2 mL PTFE holding line such that it could subsequently be pumped to the GLS at a higher flow rate of 4.6 mL min⁻¹ to enhance sensitivity, as noted earlier. The peak height of the transient signal was recorded. Despite a small initial increase in signal with increasing NO₃-, response decreased significantly with higher nitrate concentration. No explanation can be offered for this initial increase at this time, further investigation is required.

However, it may be similarly connected with a change in the identity of the Co species formed, as was noted for the case of Se (IV) when the concentration of NO₃⁻ in samples was varied.⁴⁷

In contrast to the above impact of added nitrate anion, the effect of the presence of two major metal ions on generation efficiency, Fe and Cu, was also examined. Figure 10A illustrates their influence on response from a 100 μ g L⁻¹ Co (II) standard solution and Figure 10B shows the effect these elements have on a real solution of acid digested TORT-3 CRM. The signal from the standard solution containing 0.05% nitrate (arising from the Co(NO₃)₂ stock solution used for spiking) was 32700 cps. Sequentially spiking the sample with increasing amounts of Fe and Cu derived from their stock solutions prepared in dilute HNO₃ incrementally increased the total NO₃⁻¹ content, necessitating sufficient HNO₃ being added to each solution to ensure that the concentration of this interferent was maintained constant in all of them. Thus, the initial nitrate concentration in the 100 μ g L⁻¹ Co (II) standard increased to 0.13% and response increased to 41500 cps. Addition of Cu significantly decreased response; the influence of Fe was less drastic, but it is clear that both metal ions pose problems for accurate analysis.

According to Figure 10B, similar effects were obtained when these metals were added to digests of TORT-3 (0.25 g dissolved in 10 mL 0.5% HNO₃, followed by a 5-fold dilution with pH buffered 50% formic acid). The concentrations of Cu and Fe in the digested sample of this CRM tissue (mass fractions of 497 and 179 mg kg⁻¹, respectively) yield levels of approximately 2.5 and 0.9 mg L⁻¹, respectively, in the diluted solution digests subjected to analysis. As the Co response for this real solution was low (1490 cps) due to matrix interferences and the low Co concentration ($\sim 5~\mu g~L^{-1}$) in the diluted digest, it was therefore spiked with 100 $\mu g~L^{-1}$ Co, thereby increasing the signal to 12570 cps. Addition of Cu decreased the signal drastically (as with a calibration solution) whereas addition of Fe did not significantly change the signal, possibly due to the presence of organic compounds in the digest and their potential binding of Fe.

Analysis of Reference Materials

 The analytical performance of the proposed method for the determination of cobalt was initially evaluated under the established optimized conditions, i.e., using continuous mode for

sample introduction in a medium of pH buffered 50% formic acid (Table 3). Unfortunately, no response from Co was obtained under these conditions when digested samples of TORT-2 and TORT-3 were processed due to the complexity of the resultant matrix (i.e., interferences from nitrate, Cu, Fe and possibly other elements as well as residual undigested molecular species). Subsequent experiments based on the segmented mode of sample introduction (1 mL) were undertaken to further discern the nature of the problem and means of circumventing it. Digests of TORT-3 were spiked with 100 μ g L⁻¹ Co (II) to ensure adequate signal intensity and the impact of increasing dilution with buffered formic acid examined. A sample flow rate of 0.55 mL min⁻¹ to the photoreactor yielded a photolysis time of 82 s and a total of 109 s for delivery to the holding line, after which the sample was rapidly transferred to the GLS at 4.5 mL min⁻¹. Based on recovery, the optimum dilution factor (trade-off between increased response at lower interferent concentrations and decreased signal due to dilution) of the digest solution was determined to be 5, yielding a response of 2670 cps. By comparison, the 100 μ g L⁻¹ Co standard solution in pH buffered 50% formic acid produced approximately 30000 cps under the same measurement conditions (20% lower than for continuous mode).

Three 0.26 g subsamples of TORT-2 (certified Co mass fraction of 0.51 mg kg⁻¹) were independently digested, combined and evaporated such as to yield a final solution of higher concentration of Co while maintaining a residual nitric acid concentration of 0.5%. This digest was then diluted 10-fold in 0.5% HNO₃ and a further 15-fold in pH buffered 50% formic acid, yielding a residual and constant added nitrate concentration of 0.058% to minimize interference from this species. The method of additions (two spikes) was used for quantitation along with a segmented mode of sample introduction. The slopes of the additions curves for similarly prepared samples of TORT-2 and TORT-3 differed by 10%, with greatest suppression of response occurring with digests of TORT-3, likely a consequence of its significantly higher endogenous concentrations of Cu and Fe. Furthermore, the slopes of the additions curves were 35% lower than that arising from a matrix free external calibration solution. Nevertheless, analytical results of 0.45 mg kg⁻¹ and 1.05 mg kg⁻¹ Co were obtained for TORT-2 and 3, respectively, using the method of additions, in good agreement with the expected values of 0.51 and 1.06 mg kg⁻¹, respectively, in these two biological materials.

Clearly, matrices arising from the digestion of biological tissues may cause severe interference with the process of PVG of Co, requiring use of the method of additions for analysis combined with optimized irradiation times and adequate sample dilution (to provide adequate sensitivity and precision).

Conclusions

A high efficiency PVG methodology based on the coupling of a flow-through lamp with ICP-OES detection was demonstrated for efficient generation of volatile cobalt species. The higher UV intensity from this source as well as the availability of deep UV radiation (184 nm) permits significantly reduced photolysis times (10 s in continuous mode of sample introduction for a clean sample matrix). A glass frit GLS providing enhanced sparging capability ensures high phase separation efficiency for the volatile species and improved precision. Best response was obtained using 50% formic acid buffered to pH \sim 3.3 by addition of NaOH. With continuous mode sample introduction, response increases with sample flow rate, permitting flows higher than 3 mL min⁻¹. Correlation coefficients for linear regression of calibration functions were better than 0.99, and precisions of typically 3% (RSD) provided a LOD of 0.4 μ g L⁻¹. Generation efficiency was 42%, the highest reported to date.

Unfortunately, application of this methodology to real samples, such as digested biological tissues, suffers from several matrix interferences which could not be circumvented through experimental optimization. Segmented mode of sample introduction, which decoupled the rate of introduction of sample into the PVG reactor (hence irradiation time) from that for delivery to the GLS, demonstrated that interferences could be reduced with longer irradiation times while sensitivity could be maintained using high delivery flow rates to the GLS. Good accuracy (90% to 110%) and precision (<5% RSD) were obtained for analyses of CRMs TORT-2 and TORT-3 using standard additions calibration for quantitation combined with an adequate dilution factor for the digested solution (> 50-fold dilution of the solid) and a sample flow rate of 0.5 - 1 mL min⁻¹ for segmented mode of sample introduction.

These results demonstrate that the PVG technique is not as robust as desired for applications to real samples (geological or biological samples), and experimental conditions for each matrix likely require optimization. Interferences arising from nitrate and concomitant trace elements contribute to these problems, requiring processing of all samples in an identical manner; cooling of the UV source and concomitant decreased UV output may present an additional, but untested variable.

Acknowledgement

H. C. J. is grateful for the technical support received from the Chemical Metrology Group, Measurement Science and Standards, NRC-Canada, particularly acknowledging the help of I. Pihillagawa Gedara, as well as guest worker G. S. Lopes for ICP-OES and ICP-MS analyses, respectively. He is also thankful for the scholarship sponsored by the Brazilian government (Science Without Borders program - CNPq, No. 246801/2012-3) and the Federal University of Espírito Santo (UFES) for additional financial support.

References

- [1] P. Wu, L. He, C. Zheng, X. Hou and R. E. Sturgeon, *J. Anal. At. Spectrom.*, 2010, **25**, 1217-1246.
- [2] J. Dedina and D. L. Tsalev, *Hydride Generation Atomic Absorption Spectrometry*, John Wiley & Sons: New York, 1995.
- [3] A. S. Luna, R. E. Sturgeon and R. C. Campos, *Anal. Chem.*, 2000, **72**, 3523-3531.
- [4] T. Nakahara, Spectrochim. Acta Rev., 1991, 14, 95-109.
- [5] A. Sanz-Medel, M. C. Valdés-Hevia y Temprano, N. B. García and M. R. Fernández de la Campa, *Anal. Chem.*, 1995, **67**, 2216-2223.
- [6] Y. Cai, S. Rapsomanikis and M. O. Andreae, J. Anal. At. Spectrom., 1993, 8, 119-125.
- [7] R. E. Sturgeon, S. N. Willie and S. S. Berman, *Anal. Chem.*, 1989, **61**, 1867–1869.
- [8] Y. M. Liu, B. L. Gong and T. Z. Lin, Chin. J. Anal. Chem., 1984, 12, 21–24.
- [9] M. Norman, V. Bennett, M. McCulloch and L. Kinsley, J. Anal. At. Spectrom., 2002, 17, 1394-1397.
- [10] R. E. Sturgeon and Z. Mester, *Appl. Spectrosc.*, 2002, **56**, 202A-213A.
- [11] E. Niedobová, J. Machát, V. Otruba and V. Kanicky, J. Anal. At. Spectrom., 2005, **20**, 945–949.
- [12] Y.-L. Feng, J. W. Lam and R. E. Sturgeon, *Analyst*, 2001, **126**, 1833-1837.
- [13] P. Pohl and B. Prusisz, Anal. Bioanal. Chem., 2007, **388**, 753-762.
- [14] F. Laborda, E. Bolea, and J. R. Castillo, Anal. Bioanal. Chem., 2007, 388, 743–751.
- [15] A. S. Ribeiro, M. A. Vieira S. Willie and R. E. Sturgeon, *Anal. Bioanal. Chem.*, 2007, **388**, 849-857.
- [16] Y. He, X. Hou, C. Zheng and R. E. Sturgeon, Anal. Bioanal. Chem., 2007, 388, 769-774.
- [17] Y. Yin, J. Liu, J. and G. Jiang, *Trends Anal. Chem.*, 2011, **30**, 1672-1684.
- [18] R. E. Sturgeon and P. Grinberg, J. Anal. At. Spectrom., 2012, 27, 222-231.
- [19] P. Grinberg, Z. Mester, R. E. Sturgeon and A. Ferretti, J. Anal. At. Spectrom., 2008, 23, 583–587.
- [20] X. Guo, R. E. Sturgeon, Z. Mester and G. J. Gardner, *Anal. Chem.*, 2004, **76**(, 2401-2405.
- [21] M. García, R. Figueroa, I. Lavilla and C. Bendicho, J. Anal. At. Spectrom., 2006, 21, 582–587.
- [22] C. Zheng, R. E. Sturgeon, C. Brophy and X. Hou, Anal. Chem., 2010, 82, 3086-3093.
- [23] J. A. Nóbrega, R. E. Sturgeon, P. Grinberg, G. J. Gardner, C. Brophy and E. E. Garcia, *J. Anal. At. Spectrom.*, 2011, **26**, 2519-2523
- [24] R. E. Sturgeon, S. N. Willie and Z. Mester, J. Anal. At. Spectrom., 2006, 21, 263-265.
- [25] Y. C. Sun, Y. C. Chang and C. K. Su, *Anal. Chem.*, 2006, **78**, 2640-2645.

- [26] D. Qin, F. Gao, Z. Zhang, L. Zhao, J. Liu, J. Ye, J. Li and F. Zheng, *Spectrochim. Acta Part B,* 2013, **88**, 10-14.
- [27] H. Deng, C. Zheng, L. Liu, L. Wu, X. Hou, and Y. Lv, *Microchem. J.*, 2010, **96**, 277-282.
- [28] C. Zheng, R. E. Sturgeon, C. S. Brophy, S. He and X. Hou, *Anal. Chem.*, 2010, **82**, 2996-3001.
- [29] C. Zheng, R. E. Sturgeon and X. Hou, J. Anal. At. Spectrom., 2009, 24, 1452–1458.
- [30] P. Grinberg and R. E. Sturgeon, Spectrochim. Acta Part B, 2009, 64, 235-241.
- [31] P. Grinberg and R. E. Sturgeon, J. Anal. At. Spectrom., 2009, 24, 508-514.
- [32] R E. Sturgeon, Anal. Chem., 2015, 87, 3072-3079.

- [33] T. Suzuki, R. E. Sturgeon, C. Zheng, A. Hioki, H. Tao and T. Nakazato, *Anal. Sci.*, 2012, **28**, 807-811.
- [34] A. de Jesus, R. E. Sturgeon, J. Liu and M. M. da Silva, *Microchim. J.*, 2014, **117**, 100 105.
- [35] Z. Zhu, D. He, C. Huang, H. Zheng, S. Zhang and S. Hu, *J. Anal. At. Spectrom.*, 2014, **29**, 506 511.
- [36] Y. Gao, R. E. Sturgeon, Z. Mester, X. Hou, C. Zheng and L. Yang, **Anal. Chem.**, 2015, 85, 7996 8004.
- [37] Y. Gao, M. Xu, R. Sturgeon, Z. Mester, Z. Shi, R. Galea, P. Saull and L. Yang, *Anal. Chem.*, 2015, **87**, 4495 4502.
- [38] Y. Cai, S.-H. Li, S. Dou, Y.-L. Yu and J.-H. Wang, *Anal. Chem.*, 2015, **87**, 1366 1372.
- [39] H. Duan, Z. Gong and S. Yang, J. Anal. At. Spectrom., 2015, **30**, 410 416.
- [40] C. Zheng, Y. Li, Y. He, Q. Ma and X. Hou, J. Anal. At. Spectrom., 2005, 20, 746-750.
- [41] X. Hou, X. Ai, X. Jiang, P. Deng, C. Zheng and Y. Lv, *Analyst*, 2012, **137**, 686–690.
- [42] R. E. Sturgeon and V. Luong, J. Anal. At. Spectrom., 2013, 28, 1610-1619.
- [43] R. N. Collins and A. S. Kinsela, *Chemosphere* 2010, **79**, 763-904.
- [44] D. G. Barceloux, Clin. Toxicol. 1999, **37**, 201-216.
- [45] J. R. Roth, J. G. Lawrence and T. A. Bobik, *Microbio.*, 1996, **50**, 137-181.
- [46] T. Nakazato and H. Tao, Anal. Chem., 2006, 78, 1665-1672.
- [47] X.-M. Guo, R. E. Sturgeon, Z. Mester and G. J. Gardner, Anal. Chem., 2003, 75, 2092-2099.
- [48] X.-M. Guo, R. E. Sturgeon, Z. Mester and G. J. Gardner, *Environ. Sci. Technol.* 2003, **37**, 5645-5650.
- [49] M. A. Vieira, A. S. Ribeiro, A. J. Curtius and R. E. Sturgeon, *Anal. Bioanal. Chem.*, 2007, **388**, 837-847.
- [50] X.-M. Guo, R. E. Sturgeon, Z. Mester and G. J. Gardner, *Appl. Organomet. Chem.*, 2004, **18**, 205-211.

- [51] D. B. Aeschliman, S. J. Bajic, D. P. Baldwin and R. S. Houk, *J. Anal. At. Spectrom.*, 2003, **18**, 1008-1014.
- [52] L. Flamigni, J. Koch and D. Günther, J. Anal. At. Spectrom., 2014, 29, 280-286.
- [53] Y. Gao, W. Yang, C. Zheng, X. Hou and L. Wu, J. Anal. At. Spectrom., 2011, 26, 126-132.
- [54] Y. G. Yin, J. F. Liu, B. He, S. B. Shi and G. B. Jiang, *J. Chromatogr*. A, 2008, **1181**, 77-52.
- [55] G. E. P. Box, W. G. Hunter and J. S. Hunter, *Statistics for experimenters: design, innovations and discovery*. 2ª Ed. New York: Wiley, 2005. 639 p.

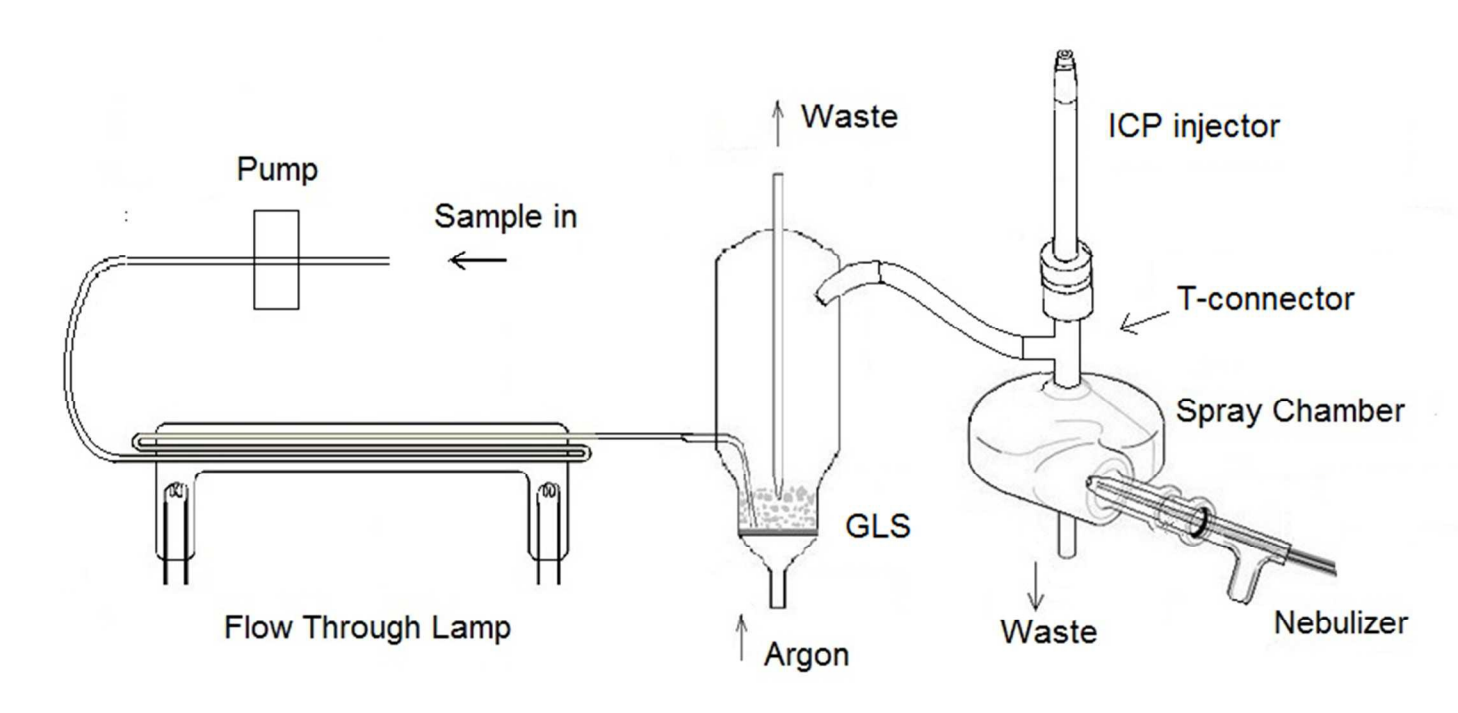


Figure 1. Schematic of the experimental setup showing flow-through PVG reactor mated to large frit GLS.

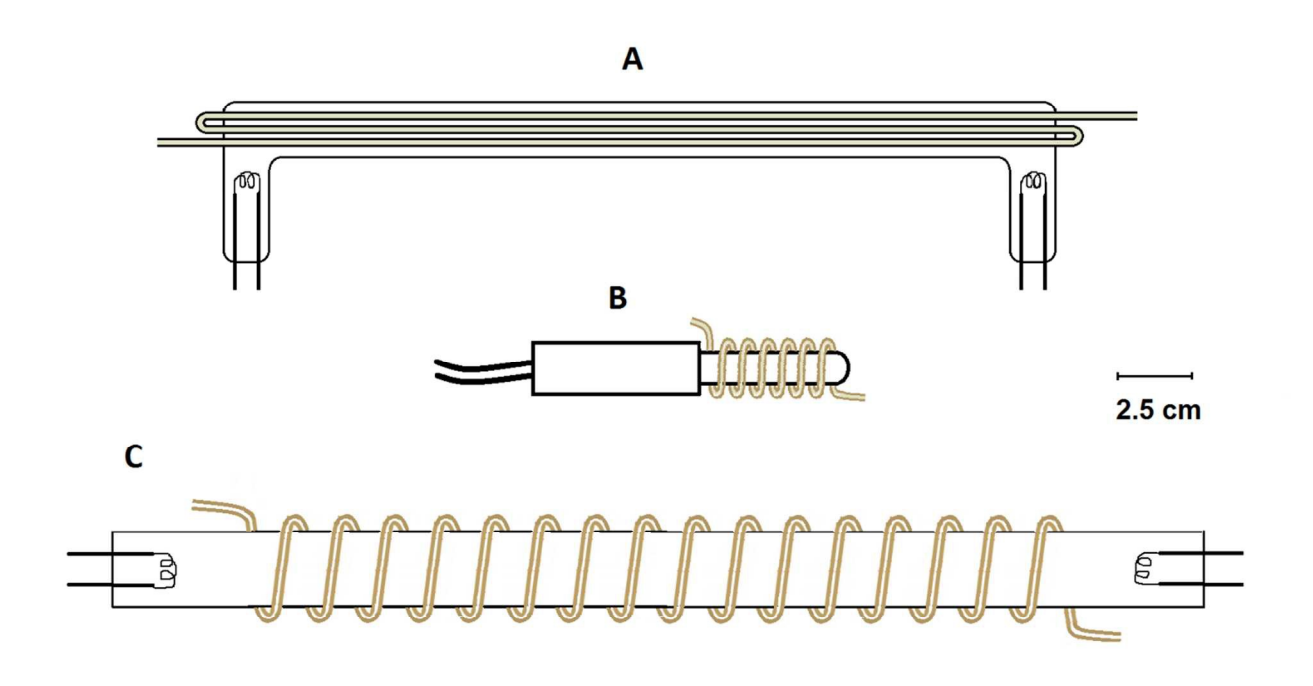


Figure 2. Different lamps used in the PVG system (to scale). A: flow-through Lamp (19 W), B: pen lamp (3 W) and C: germicidal lamp (15 W).

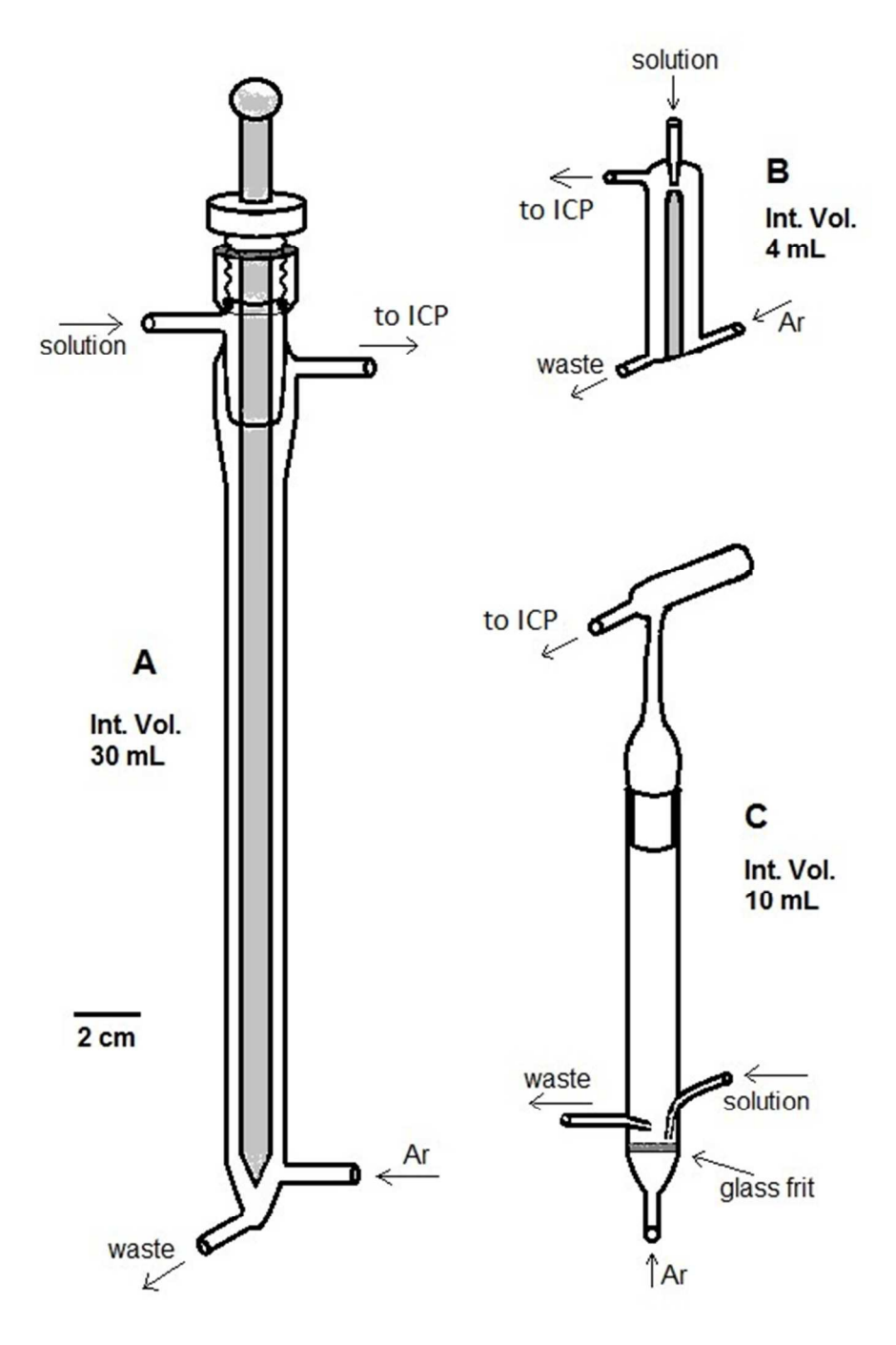
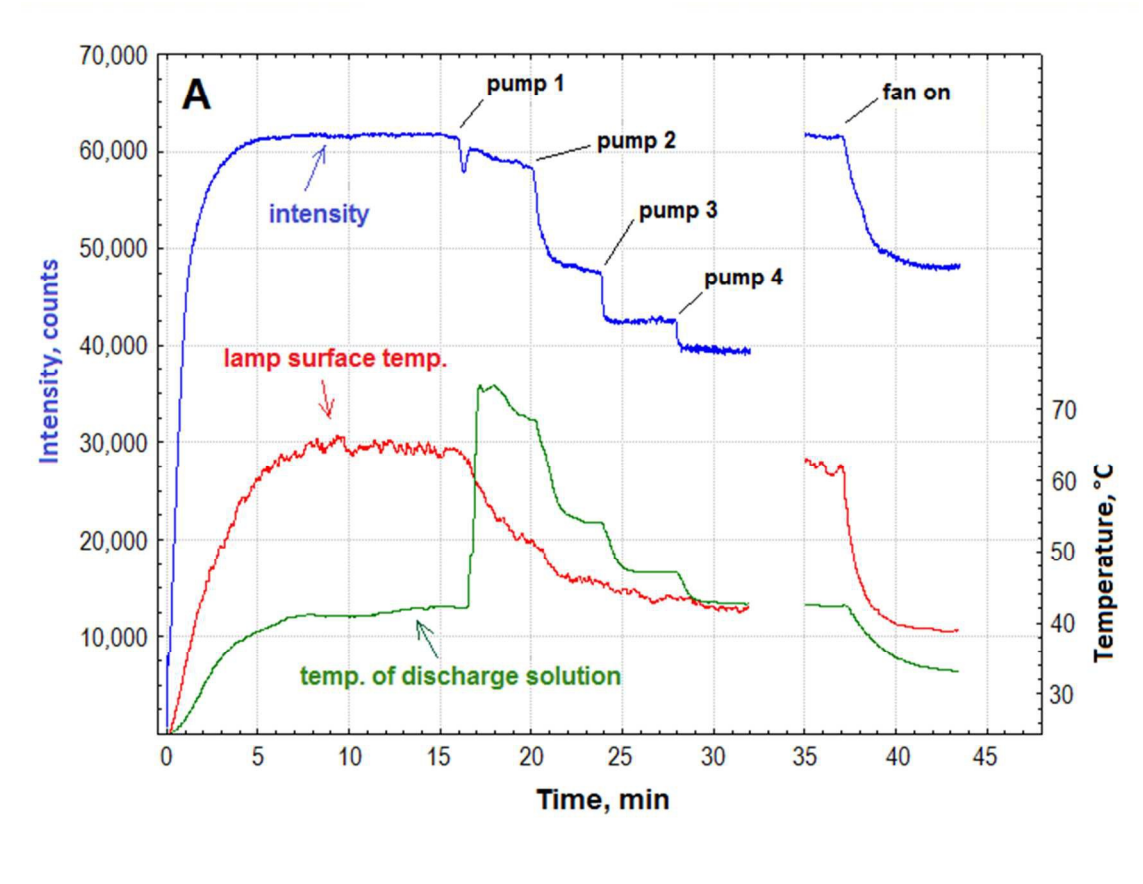
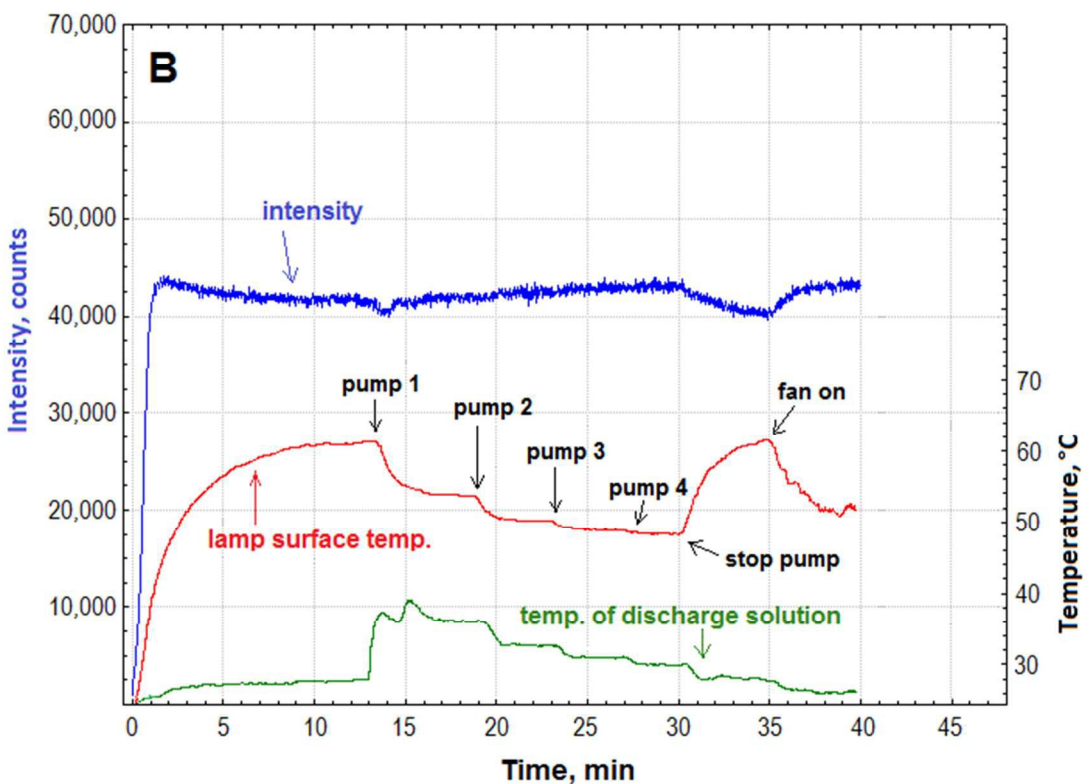


Figure 3. Alternative gas-liquid separators used in this work (to scale). **A**: passive GLS from Tekran Instruments series 2600 automated water analysis system (Toronto, Canada), **B**: Varian Instruments thin-film passive GLS and **C**: medium GLS containing supporting glass frit.





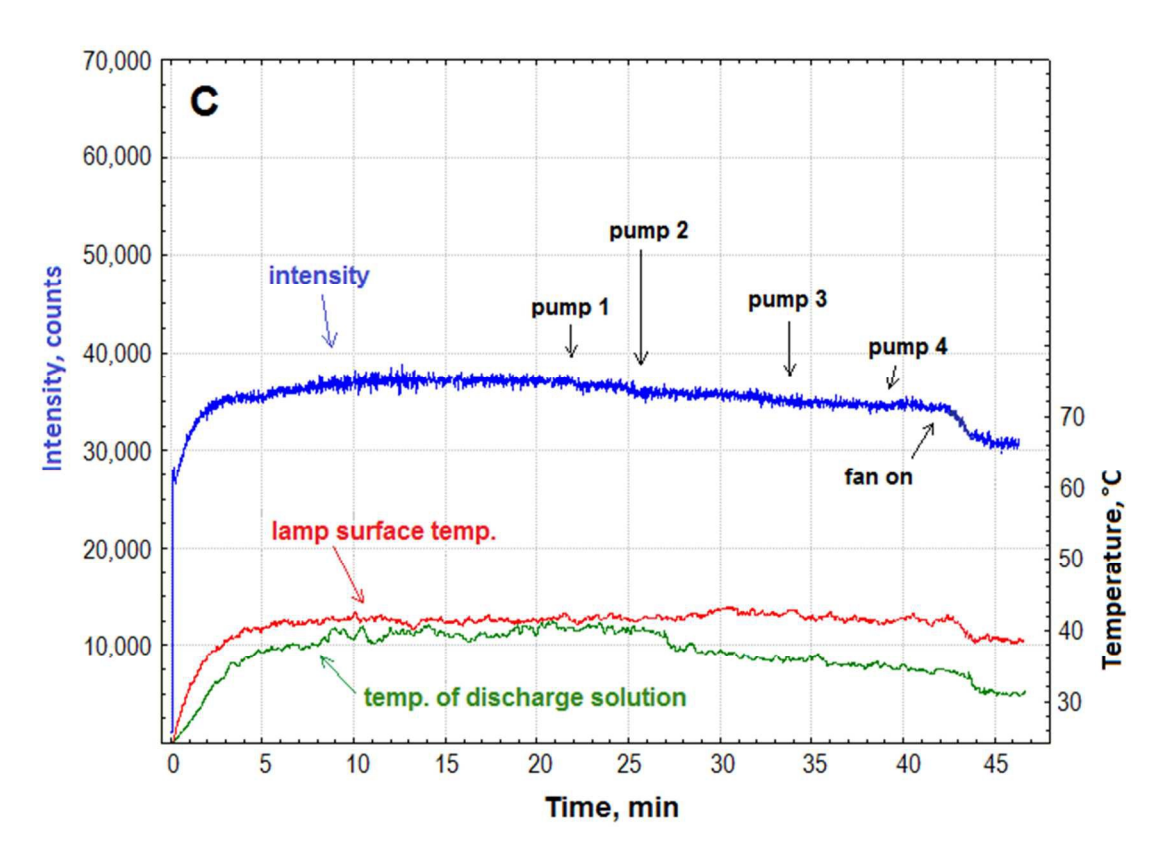


Figure 4. Temporal variation of UV intensity of the 254.52 nm Hg line and that of the temperature of both the lamp surface and water exiting each PVG system. Water flow rates: pump 1 to 4 = 1, 2, 3 and 4 mL min⁻¹, respectively. Impact of forced air surface cooling with a small fan is also shown. **A**: flow-through lamp, **B**: pen lamp and **C**: germicidal lamp.

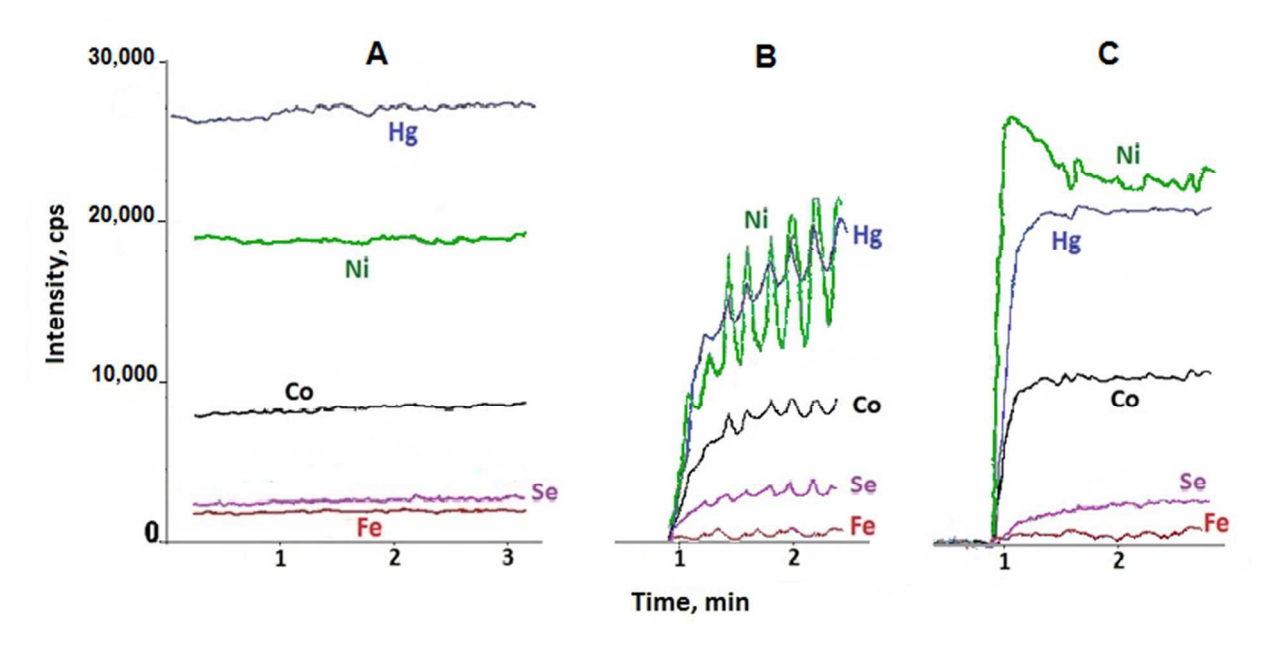


Figure 5. Temporal variation of emission intensity from a multi-element solution containing 30% formic and 20% propionic acid using the flow-through photoreactor combined with: (A) the large glass frit GLS; (B) the passive GLS and (C) the medium glass frit GLS. Generation conditions are summarized in Table 1.

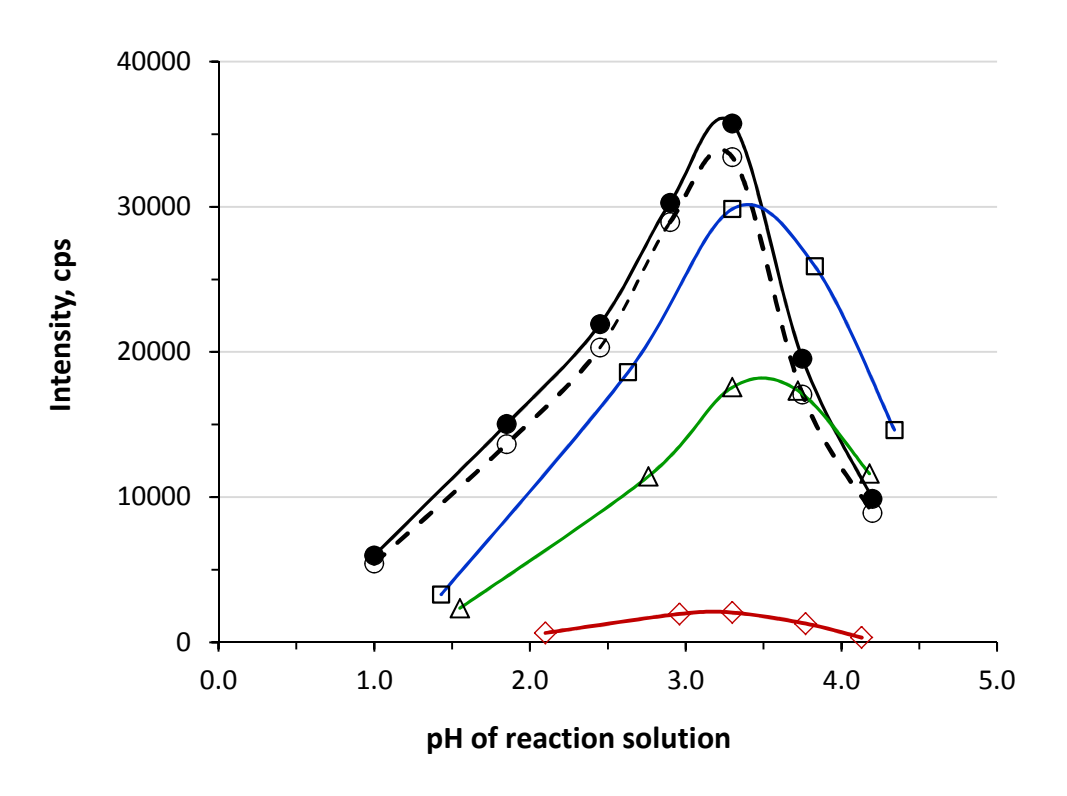


Figure 6. Effect of pH on steady-state response from pH buffered solutions containing 100 μg L⁻¹ Co(II) in varying concentrations of formic acid (% v/v). All responses recorded during simultaneous nebulization of water into the spray chamber, i.e. wet plasma, (●) 50%, (□) 30%, (△) 20% and (♦) 5% formic acid), except (O) dotted line 50% formic acid (dry plasma). Sample flow rate 3.4 mL min⁻¹ to GLS, argon flow rate through GLS = 160 mL min⁻¹, precision 1-4% RSD.

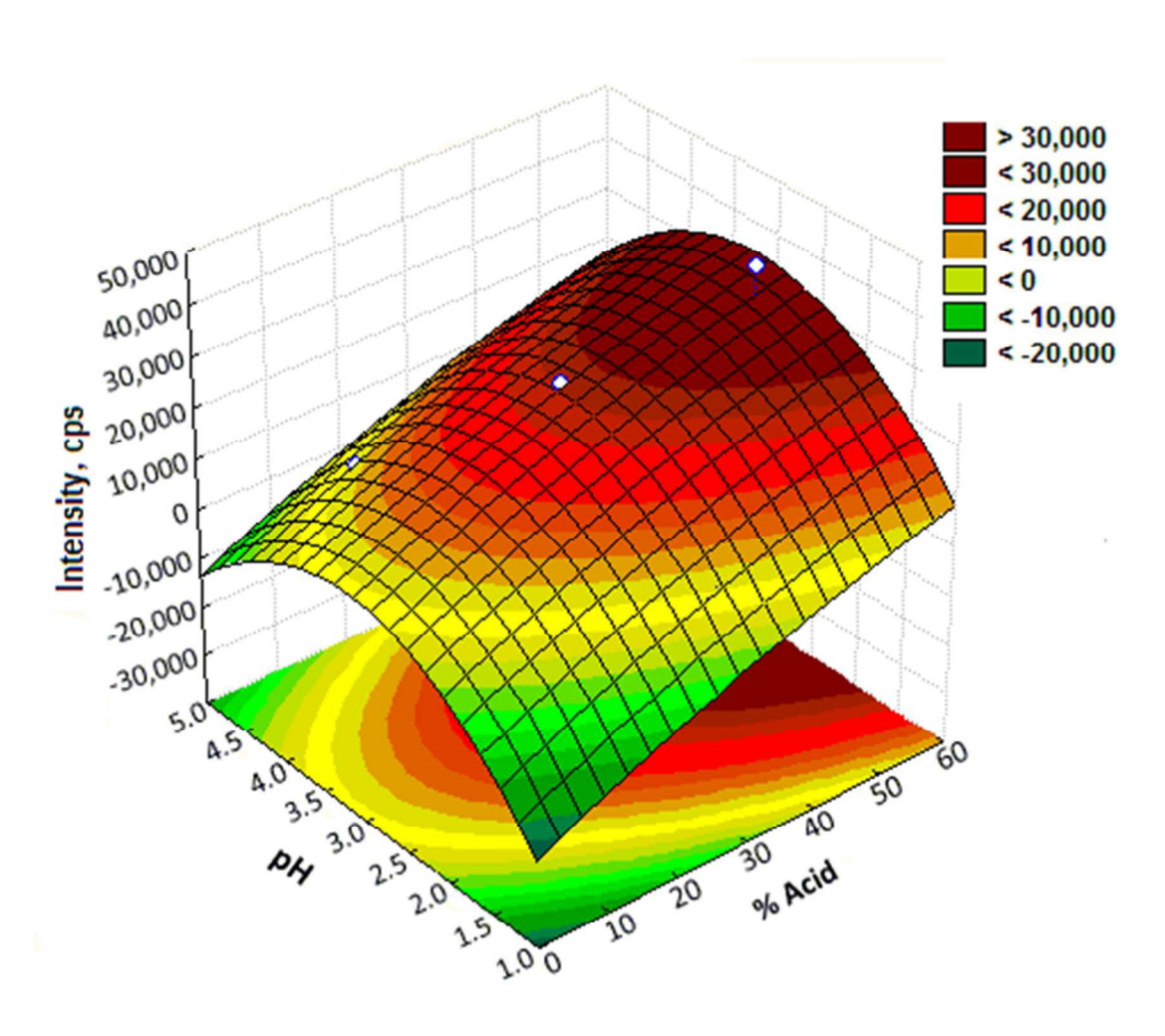
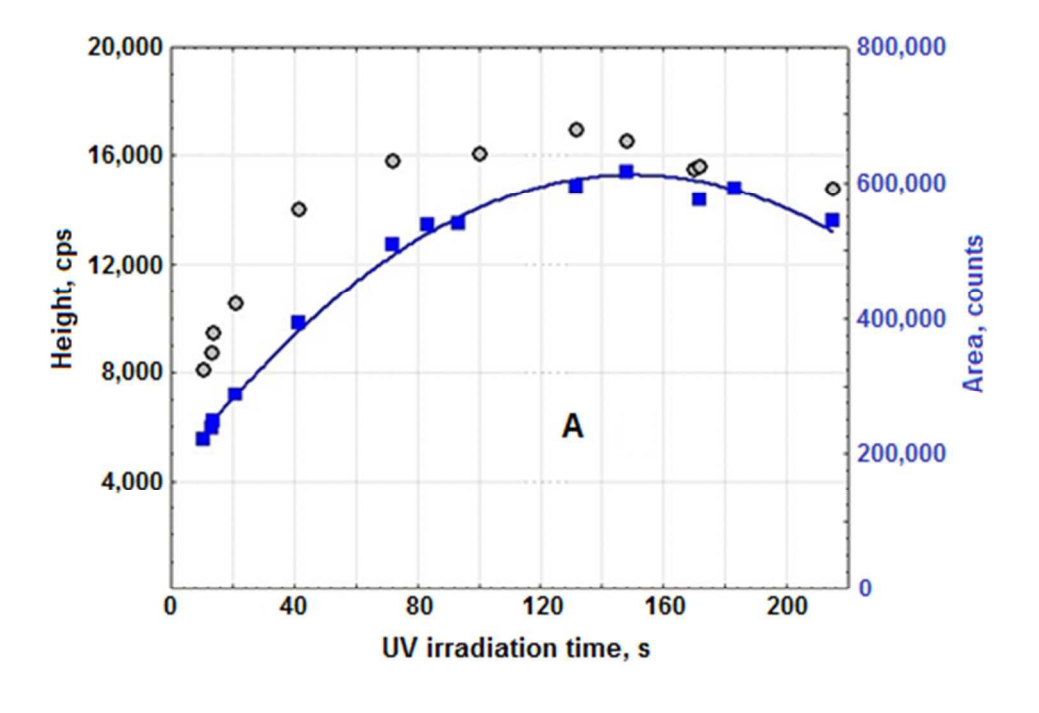


Figure 7. Estimated surface response for Co as a function of pH and formic acid concentration based on a central composite design. For a constant sample flow rate the Co intensity from a solution of 100 μ g L⁻¹ Co(II) is defined by the equation: Intensity= -68740 + 682xA -2,90xA² + 34521xpH -5372xpH² +17224, A= % acid. The blank dots are outliers.



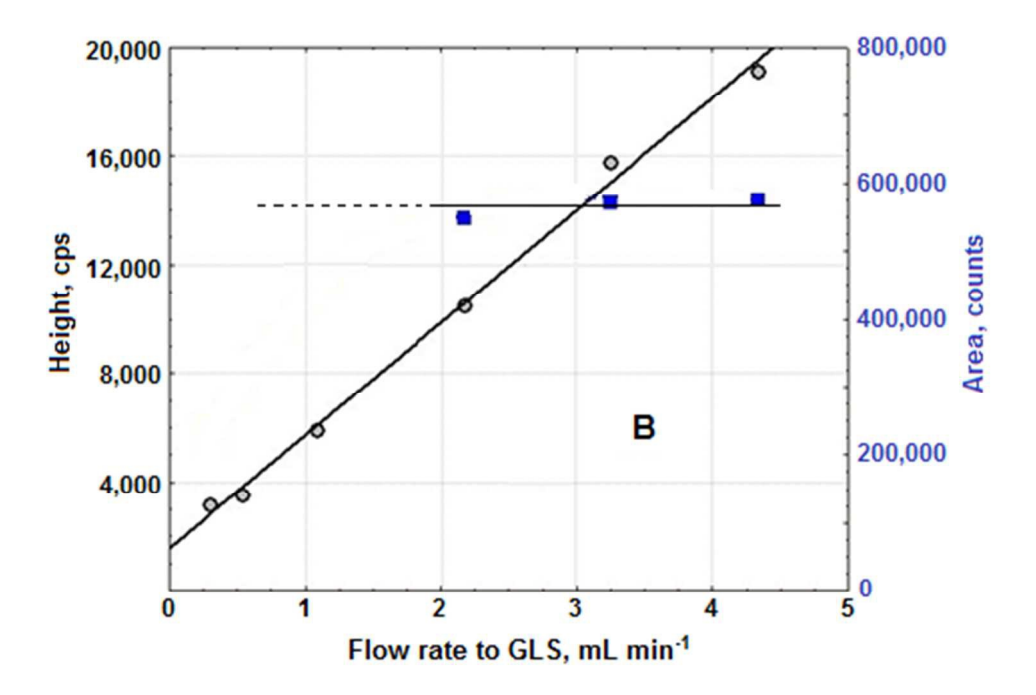


Figure 8. Segmented mode of sample introduction to the flow-through lamp. **A:** Effect of sample flow rate (hence, irradiation time) on response from pH=3.3 buffered 50% v/v formic acid containing of 100 μ g L⁻¹ Co (II). Ar flow rate through the GLS = 160 mL min⁻¹; sample flow rate to the GLS = 4.3 mL min⁻¹. **B:** Effect of sample flow rate to the GLS for a fixed 83 s irradiation time (i.e., 0.54 mL min⁻¹). Ar flow rate through the GLS = 160 mL min⁻¹. (O) peak height (precision of 1-4%) and (\square) peak area (precision of 5-10%).

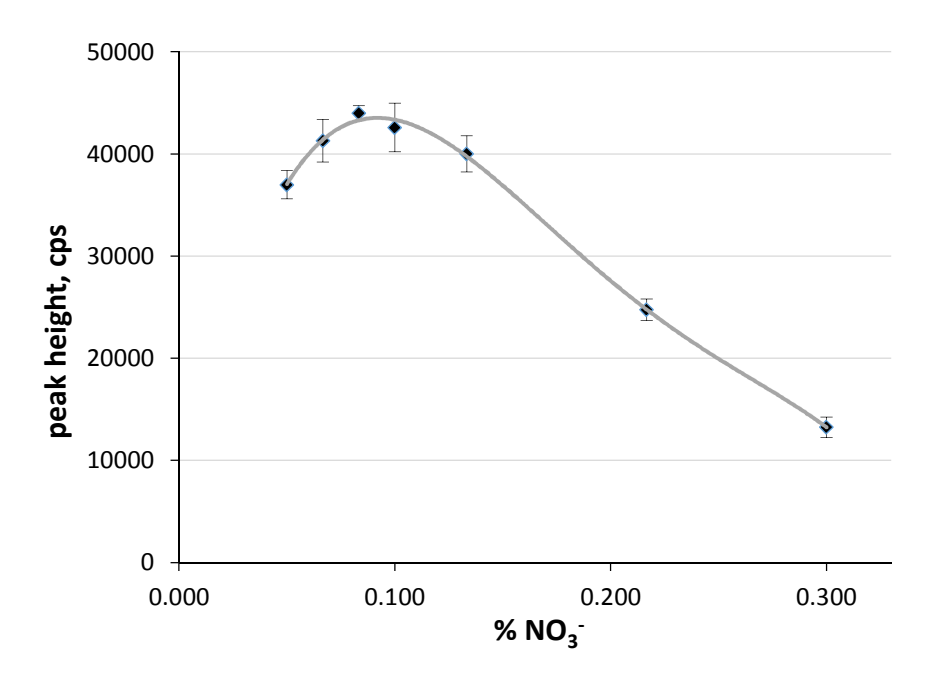


Figure 9. Effect of nitrate on response from 100 μ g L⁻¹ Co (II) in pH 3.5 buffered solution 50% formic acid. Introduction of 1 ml volume using segmented mode to flow-through lamp.

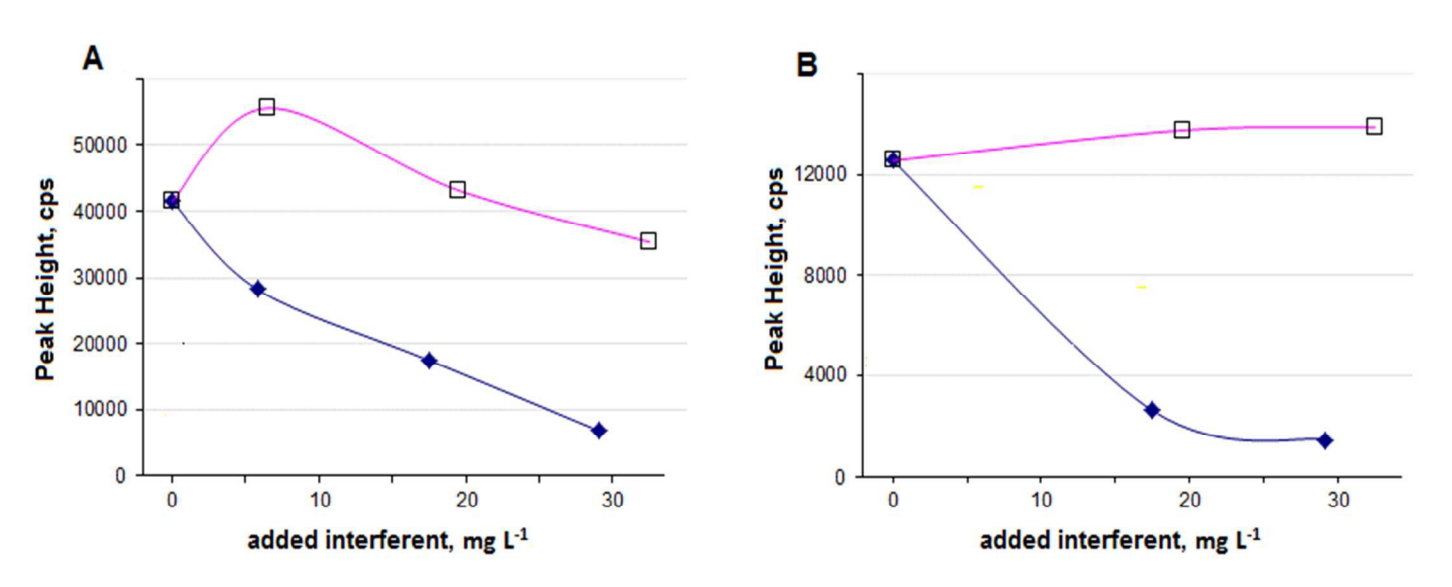


Figure 10. Interference from added (\square) Fe and (\diamondsuit) Cu on response from Co using 1 mL segmented mode sample introduction (flow rate= 1.1 mL min⁻¹). **A:** Cu or Fe added from their stock solutions (1795 and 2000 mg L⁻¹, respectively, in 5% HNO₃) into a 100 μ g L⁻¹ Co pH 3.5 buffered solution of 50% formic acid. **B:** Effect of Cu and Fe added to a solution of digested TORT-3 CRM diluted with 50% formic acid buffered to pH 3.5 and spiked with 100 μ g L⁻¹ Co. See text for further details.

Table 1. Effect of lamp type on steady-state PVG response.

Element	Hg	Se	Fe	Ni	Со
λ (nm)	253.652	196.026	259.939	231.604	238.892
(μg L ⁻¹)	100	200	200	500	500
Lamp	Response,	cps			
flow-through	26770	2510	1900	18620	8620
pen lamp	44180	180	<200	410	220
germicidal Lamp	39270	110	<200	1320	1060

Experimental conditions: ICP power= 1300 W, auxiliary gas= 0.3 L min⁻¹, nebulizer gas= 0.5 L min⁻¹, Ar flow rate to large GLS= 160 mL min⁻¹ (Figure 1), solution flow rate to lamp = 2.2 mL min⁻¹, (providing same irradiation time of 20 s for all lamps as irradiated volume was fixed at 0.75 mL). Multi-element test solution: unbuffered mixture of 30% formic and 20% propionic acids.

Table 2. Impact of lamp type on Co response.

Lamp	Solution	Volume (mL)	Flow rate (mL min ⁻¹)	Average (cps)	sd	Irradiation time (s)
Flow-through	30% pH 3.5	0.75	3.5	27100	340	13
Pen	30% pH 3.5	0.75	3.5	2020	130	13
Germicidal	30% pH 3.5	0.75	3.6	2820	100	13
Flow-through	50% pH 3.8	0.75	3.5	35000	285	13
Pen	50% pH 3.8	0.75	3.5	3700	100	13
Germicidal	50% pH 3.8	0.75	3.6	4878	100	13
Pen	30% pH 3.5	1.3	3.4	5617	100	23
Germicidal	30% pH 3.5	8.0	3.4	11481	350	141
Pen	50% pH 3.8	1.3	3.4	4738	60	23
Germicidal	50% pH 3.8	8.0	3.4	16248	250	141

Experimental conditions: ICP power= 1300 W, auxiliary gas= 0.3 L min^{-1} , nebulizer gas= 0.5 L min^{-1} , Ar flow rate to large GLS= 160 mL min^{-1} . Maximum exposed volume: Flow-through lamp = 0.75 mL, Large lamp= 8 mL and 1.5 mL to Pen lamp. Continuous mode of sample introduction of 100 µg L^{-1} Co in buffered (pH 3.5 or 3.8) formic acid media.

Table 3. Analytical figures of merit.

	50% formic acid
Sample Volume, mL	10
pH range	3.0-3.5
Calibration equation (I in cps, C in μ g L ⁻¹)	I = 375.C
Correlation Coefficient, R	0.9975
LOD, μg L ⁻¹	0.4
Precision at 100 μg L ⁻¹ , % RSD, n=10	2%
PVG efficiency, %	42 ± 2

Instrumental conditions: Continuous mode sample introduction, flow-through lamp, 60 mL glass frit GLS, rf power= 1300 W, auxiliary gas= 0.3 L min⁻¹, nebulizer gas= 0.5 L min⁻¹, Ar flow rate to GLS= 160 mL min⁻¹, PVG sample flow rate = 3.4 mL min⁻¹.

